# A Sensitivity Analysis for Power Profile Modeling
## A Case Study of Dutch DC Railway Networks

Rojas, Julian; Rivera, Sebastian; Diab, Ibrahim; Bauer, Pavol

**DOI**
10.1109/SPEEDAM61530.2024.10609083

**Publication date**
2024

**Document Version**
Final published version

**Published in**
Proceedings of the 2024 International Symposium on Power Electronics, Electrical Drives, Automation and Motion, SPEEDAM 2024

**Citation (APA)**
Rojas, J., Rivera, S., Diab, I., & Bauer, P. (2024). A Sensitivity Analysis for Power Profile Modeling: A Case Study of Dutch DC Railway Networks. In *Proceedings of the 2024 International Symposium on Power Electronics, Electrical Drives, Automation and Motion, SPEEDAM 2024* (pp. 1081-1086). IEEE. https://doi.org/10.1109/SPEEDAM61530.2024.10609083

2024 International Symposium on Power Electronics,
Electrical Drives, Automation and Motion

# A Sensitivity Analysis for Power Profile Modeling: A Case Study of Dutch DC Railway Networks

1st Julian Rojas
*Electrical Sustainable Energy department*
*Technische Universiteit Delft (TU Delft)*
Delft, The Netherlands
J.A.RojasVillarroel@tudelft.nl

2nd Sebastian Rivera
*Electrical Sustainable Energy department*
*Technische Universiteit Delft (TU Delft)*
Delft, The Netherlands
S.Rivera@tudelft.nl

3rd Ibrahim Diab
*Electrical Sustainable Energy department*
*Technische Universiteit Delft (TU Delft)*
Delft, The Netherlands
i.diab@tudelft.nl

4th Pavol Bauer
*Electrical Sustainable Energy department*
*Technische Universiteit Delft (TU Delft)*
Delft, The Netherlands
P.Bauer@tudelft.nl

2024 International Symposium on Power Electronics, Electrical Drives, Automation and Motion (SPEEDAM) | 979-8-3503-8759-9/24/$31.00 ©2024 EU | DOI: 10.1109/SPEEDAM61530.2024.10609083

***Abstract*—DC energy hubs have emerged as suitable candidates to enhance the electrical infrastructure in a localized approach, allowing future expansion in the transportation sector despite the electricity grid congestion. However, a risk in designing such a hub is that the outcome of the optimization can be a mere consequence of the (lack of) sophistication of its generation and load models. In that aim, this paper presents a sensitivity analysis for a power demand profile for a DC railway traction power substation, taking into account traction power parameters and the heating, ventilation, and air conditioning (HVAC) modeling approaches. It is found that the traction parameters such as total mass can be confidently considered using an averaged value. On the other hand, modeling the HVAC system using an averaged power demand can lead to errors over 6%, especially in the recovered braking energy calculations.**

***Index Terms*—Energy hub, energy storage, grid congestion, high power rectifiers, renewable energy, railways, traction.**

## I. Introduction

Transportation is one of the major contributors to greenhouse gas emissions and one of the main causes of climate change. In fact, the carbon footprint left behind by transport is responsible for around 20% of greenhouse gas emissions in Europe and has become a growing concern nowadays. Rail transport actually is one of the greener options in the transportation sector, especially in the Netherlands where most lines are electrified. Compared to other sectors, railway systems have a relative low carbon footprint as well. However, industry partner has set carbon neutral goals to push this even further, being also an opportunity to slow down environmental deterioration and displace fossil fuels as the dominant source of energy. Additionally, as the world becomes increasingly urbanized, the demand for transportation is expected to rise. According to the European Commission, by 2030, scheduled collective travel of under 500 kilometers should be carbon neutral within the EU, and high-speed rail traffic will be doubled. Beside the quick expansion in the labour of transport electrification and the significant increases in electric vehicle charging demand, it is estimated that the utilization of the distribution systems will reach their maximum capacity, which will further accelerate many of these challenges [1–5]. In light of the above, electric railway systems (ERS) are required to move toward greener solutions, as other rail-based means of transportation like trolleybuses or trams [6, 7]. Some researchers pointed out the potential benefits of adopting distributed energy resources (DERs) in terms of efficiency and sustainability, like renewable energy systems (RES) such as photovoltaic (PV) arrays and wind turbines, in combination with different energy storage systems (ESSs) to effectively carry out RBE or peak power shaving [8–12]. Nevertheless, the large infrastructure investments required for upgrading the railway infrastructure arise several challenges for finding suitable solutions to achieve a smoother energy transition. For further understanding, it is important to develop a mathematical model of the railway power system and provide sensitivity information regarding some assumptions and parameters considered. This paper presents a sensitivity analysis for a power profile demand model for DC railway system. The paper is structured as following. In Section II, the power profile modelling is presented. Section III presents the discussion and results for the sensitivity analysis. Finally, conclusions are listed and summarized according to the results.

## II. DC railway systems

The first electric railway in the Netherlands started to operate in 1908, Hofpleinlijn, connecting Rotterdam with the Hague and Scheveningen. Initially, it was based on an AC 10kV system, transitioned into DC in 1922. The current DC railway traction power system (TPS) in the Netherlands is based on a 1.5 kV DC network with a maximum current rating of 5200 A. A layout is depicted in Fig. 1, where a bilateral feeding between two substations, one at the left side for 24 pulse rectifier and the right side for 12 pulse rectifier, and its connection to the catenary is presented. Despite its reliability and robustness, the control capacity of the existent TPS is limited, as it can only draw power from the grid. Furthermore, diode based rectifier doesn't provide any voltage nor power control capabilities. Besides, with the expected increase in energy demand, transportation sector growth, and the congestion from the public grid side, this layout further challenges future expansions, which requires an upgrade from transmission to distribution electrical infrastructure, involving

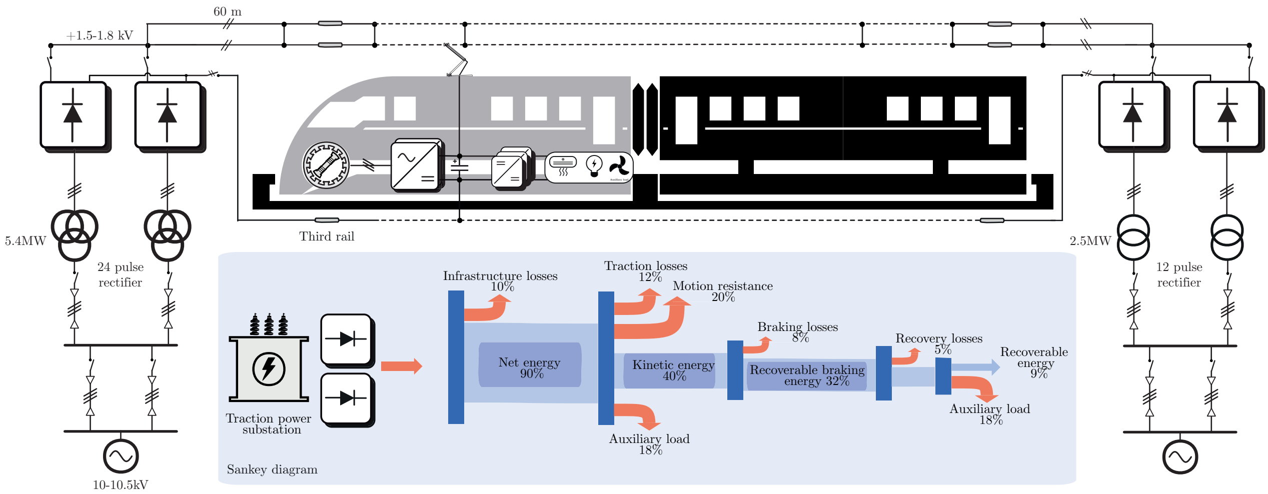


Fig. 1. DC railway power system. Energy flow in urban railway.

substantial investments that neither the public nor private sectors are willing or capable of spending. Every year, the owner of the infrastructure has to estimate the required capacity for each connection in order to settle the contracted transport power (GTV or *Gecontracteerd Transport Vermogen*, in Dutch) with the public grid operators. The agreed maximum power consumed from the grid over the last 15 minutes must be below the GTV, otherwise fines could be applied depending how severe the infraction is. Researchers have been encouraged to find suitable upgrades to the electrical infrastructure of DC railways for allowing their expansion, without compromising nor saturating the public grid [13, 14]. Similarly, as the idea of having control over the power flows between distributed energy resources within the DC power system is getting more attention, DC blocks composed by RESs and BESs emerged as a suitable candidate for overcome the above-mentioned challenges, providing energy management capabilities, reducing the energy dependence from the public grid due the local generation and storage.

## A. Rolling stock

In Fig. 1 a Sankey diagram with the main energy consumption and losses in urban railways is depicted. First, the losses related with infrastructure typically represent 10% of the total energy usage. These losses are mainly caused by transmission lines and conversion through transformer and rectification. From the 90% of the energy that goes into the train, only 40% is converted into kinetic energy, while the rest distributed among 3 main sources. Twenty percent of the energy goes to motion resistance, caused by the rolling and aerodynamic drag, other 12% goes to mechanical conversion losses due gearbox and motor efficiencies, and the auxiliary loads, which include lighting, control circuits, cabin doors, heat, ventilation and air conditioner (HVAC). The energy consumption of auxiliary loads can vary drastically, and it will depend of the season of the year and the country as well. For instance, it could vary between 15% and 40% for Scandinavian countries like Norway and Finland between summer and winter, while in the Netherlands between 10% and 30% of the total net energy. Regarding the recoverable energy available from the electrical braking, it is estimated that 8% of the remaining kinetic energy is typically wasted by over-voltage protection at the catenary level. This protection is based on a chopper resistor, which is usually engaged when the train starts braking at high speed. The remaining recoverable braking energy could vary between 9% and 27% depending on the auxiliary load consumption. For recovering energy from the brakes in urban railways, optimization measures on train operation need to be focused on, to increase the energy saving effect by improving the utilization of regenerative energy and reducing the traction energy consumption [15].

## B. Load profile modelling

In order to determinate a power demand profile for the traction power substations, a set of equations is derived from basic physics equations. Consider a train which is moving at speed $v_t$ like the one presented in fig: 2. By fundamental mechanical force laws, the main forces involved in the model are the traction force, the rolling resistance, and the aerodynamic drag. The following set of equations describes the main forces respectively.

$$
\begin{aligned}
F_t &= m_t \cdot a_t + F_r + F_w \\
F_r &= \alpha_r \cdot m_t \cdot \mathrm{g}\cos(\theta) + \alpha_r \cdot m_t \cdot \mathrm{g}\sin(\theta) \\
F_w &= \frac{1}{2} C_w \cdot A \cdot \rho \cdot v_t^2
\end{aligned}
\tag{1}
$$

Where $m_t$ is the weight of the train, $v_t$ is the traveling speed, $\alpha_r$ is the friction factor, g is the gravitational constant, $C_w$ , $A$ and $\rho$ are drag coefficient, front area of the train and air density, respectively. Normally, finding these parameters can be difficult, and it will depends on the characteristics

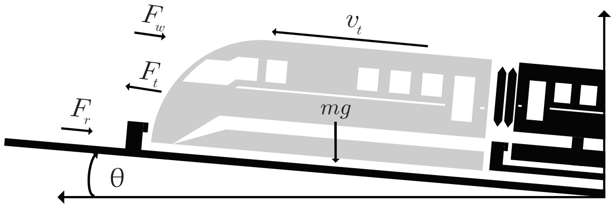


Fig. 2. Free body diagram of an urban railway.

of each train, the material of the wheels and rails, and the air characterisation. One of the resistance components mainly depends on the speed of the train, and, on the other hand, the rolling resistance depends on the mass, gravity and the gradient. Considering that the surface in the Netherlands mostly flat, the rolling resistance could be approximated as a constant. The sum of both resistance forces can be described by the Davis equation, as a second order polynomial function as the following expression:

$$F_r + F_w \approx \alpha \cdot v_t^2 + \beta \cdot v_t + \gamma$$

Lastly, considering the mechanical conversion efficiency as $\eta_m$, the power demand of a train traveling at speed $v_t$ can be describe by the following equation.

$$\begin{aligned} P_t &= v_t \cdot F_t \cdot \eta_m \\ P_t &\approx v_t \cdot (m_t \cdot \frac{\mathrm{d}v_t}{\mathrm{d}t} + \alpha \cdot v_t^2 + \beta \cdot v_t + \gamma) \end{aligned} \tag{2}$$

Where $P_t$ is the traction power demanded, $\alpha$, $\beta$ and $\gamma$ are the coefficients used for characterize the resistance force for the given train.

### C. Auxiliary load

The auxiliary load takes around $20-30\%$ of the total energy consumption, which is divided into lightning, HVAC and auxiliaries and control circuits like USB chargers and cabin doors. In several traction modelling approaches, auxiliaries are considered as a constant power load, which, can be an accurate approximation for lights and controllers which are rated at $10-15\%$ of the total auxiliary load, however, HVAC are normally controlled by on-off logic, either hysteresis or timers. The remaining $80-85\%$ of the total power demand can be described by a pulse train as it shown in the following expression.

$$H(t) = \begin{cases} \hat{P}_{\text{HVAC}} & \text{if } t \leq DT,\, D \leq 1\, \forall t \in [0, T] \\ 0 & \text{otherwise} \end{cases}$$

This equation serves as an ideal representation, however since it non-linear and non-differentiable nature in a continuous domain. It derivative can be expressed as a train of impulses or Dirac deltas, nevertheless, an analytical approximation is presented in Eq. 3.

$$H(t) \approx \frac{1}{1+e^{-kt}} \tag{3}$$

$$\frac{\mathrm{dH(t)}}{\mathrm{dt}} \approx \frac{ke^{kt}}{(e^{kt}+1)^2} \tag{4}$$

### D. Catenary modeling

As mentioned earlier, the rolling stock can be modeled as a load that is moving along the catenary. The position of the train will also impact the variation on the equivalent resistance between the TPS and the train, given by the characteristic impedance of the catenary and the distance between them. The impedance per kilometer of the catenary and the third rail are known parameters. Furthermore, since the DC characteristic predominates in the system, capacitance and inductance properties of the lines can be neglected, although, in transient analysis may be necessary. Based on the next set of equations, the model describes the catenary equivalent resistance from each substation $i$,$j$ connected to a train at certain distance at a given moment.

$$\begin{aligned} x_k(t) &= \int_{t_0}^{t} v_k(t)\, dt + x_{k_0} \\ Z_{i_i} &= Z_l \cdot |x_k| + Z_{i_f} \\ V_{L_k} &= V_i - I_{i_i} \cdot Z_{i_i} - Z_{i_f} \cdot \sum_{k=i}^{n} I_{i_k} \\ V_{L_k} &= V_j - I_{j_i} \cdot Z_{j_i} - Z_{j_f} \cdot \sum_{k=j}^{n} I_{j_k} \end{aligned} \tag{5}$$

Where $x_k$ is the train position, $x_{k_0}$ is the initial position of a train respect to the substation $i$, $Z_{i_i}$ is the equivalent impedance from the substation $i$ to the train position within the catenary $i$, $Z_l$ is the characteristic impedance of the line in Ω/km, and $I_{i_i}$ is the current flowing from the substation $i$ toward the catenary branch $i$.

### E. Substation demand profile

The power substation can be modeled as a DC voltage source connected in series with a diode and a feeder cable. The DC voltage and the feeder resistance can be calculated by Thévenin equivalence. The connection between the feeder cable and each one of the catenary is through a switch per pole for protection, modeled as part of the resistance of the feeder cable.

Given the speed of the train, the power required for the mechanical force can be calculated. An equivalent circuit is presented in Fig. 1.

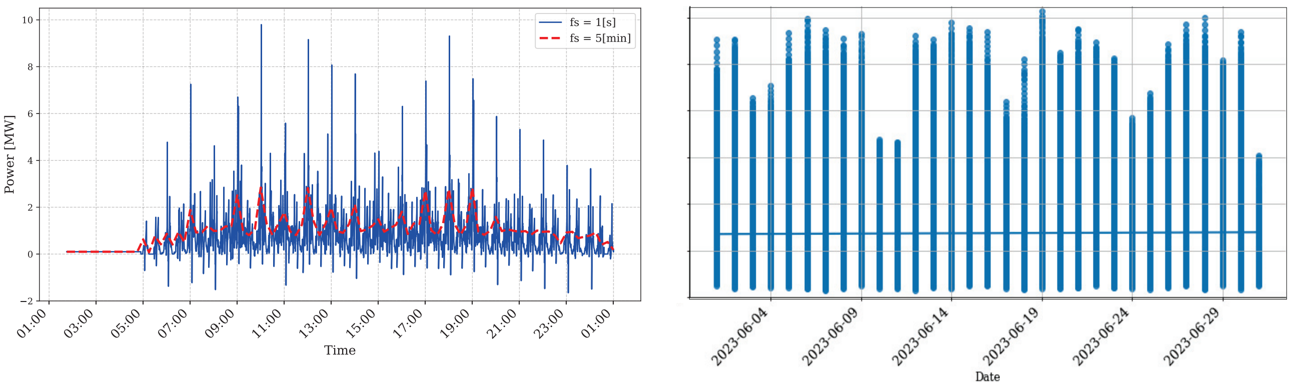


Fig. 3. Power consumption profile for Almelo, June 2023.

$$
\begin{aligned}
P_{Li} &= P_{ti} + P_{aux_i} \\
I_{L_i} &= \frac{P_{Li}}{V_{Li}} \\
V_i - Z_{i_i} \cdot I_{i_i} &= V_{Li} \\
V_j - Z_{j_i} \cdot I_{j_i} &= V_{Li} \\
I_{j_i} &= I_{i_i} \cdot \frac{Z_{i_i}}{Z_{j_i}} \quad \text{if } V_i = V_j \\
I_{j_i} &= \frac{I_{i_i} \cdot Z_{i_i} - \Delta V_{i-j}}{Z_{j_i}} \quad \text{if } V_i \neq V_j
\end{aligned} \tag{6}
$$

Where $I_{L_i}$ is the current in the pantograph, $\Delta V_{i-j}$ is the difference of voltage between substation $i$ and $j$, $P_{L_i}$ is the DC power of the train connected to the catenary $i$, $P_{t_i}$ and $P_{aux_i}$ are the traction and auxiliary power demand for that specific train. Note that if the system is perfected balanced, the equation dictates that the power split among both substations only depends on the distance ratio between them. The previous set of equations characterize the power demand profile for a particular substation. Simulation results for Almelo, Overijssel, in June 2023 are presented in Fig. 3. It is noticeable, that in order to evaluate a specific power substation within the railway power system, each one of the segments fed by the substations has to be properly identified and merged with the

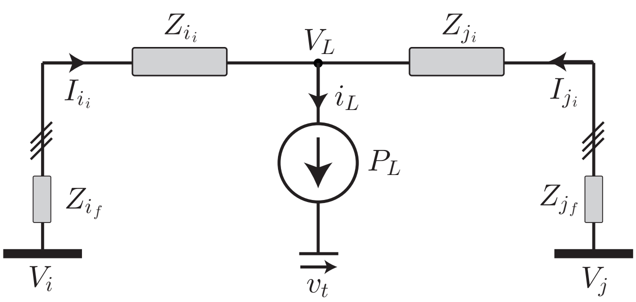


Fig. 4. Equivalent power circuit for a bilateral power system model.

information from the timetable. For each trip, a random speed profile is generated based on 3 states, acceleration, cruise, and braking periods. Efficient driving strategies like coasting are not considered. Depending on the distance between the departure and arrival points, and the constraints given by the train characterization, the acceleration/braking slope can be calculated, thus, the speed profile for the specific trip is obtained, therefore, the DC power demand of the train. Note that each trip can have several stops before arriving to destination, where the power consumption of the train will be only given by the auxiliary load, since is stopped in the station. Finally, the power demanded from a substation $i$ can be calculated as eq. 7.

$$
P_{SS_i} = \sum_{k}^{n} V_i \cdot I_{i_k} \tag{7}
$$

## III. Discussion and Results

### A. Parameter sensitivity

In order to evaluate the effect of the parameters from eq. 2, the expression is derived as following.

$$
\begin{aligned}
\frac{\partial P_L}{\partial t} &\approx 3\alpha \cdot v_t^2 \cdot a_t + 2\beta \cdot v_t \cdot a_t + \gamma \cdot a_t + m_t(a_t^2 + v_t \cdot \frac{\partial a_t}{\partial t}) \\
\frac{\partial P_L}{\partial m_t} &\rightarrow v_t \cdot a_t + v_t(\frac{\partial \gamma}{\partial m_t} + \frac{\partial \beta}{\partial m_t}) \\
\frac{\partial P_L}{\partial \alpha} &\rightarrow v_t^3 \cdot \frac{\partial \alpha}{\partial v_t} \\
\frac{\partial P_L}{\partial \beta} &\rightarrow v_t^2 \cdot \frac{\partial \beta}{\partial v_t} \\
\frac{\partial P_L}{\partial \gamma} &\rightarrow v_t
\end{aligned} \tag{8}
$$

The variation of the parameters $\alpha$ and $\beta$ are correlated with the aerodynamic drag force of the environment and the air characterization. On the other hand, $\gamma$ is related to the mechanical friction between rails and wheels. Normally, these parameters don't vary significantly, however, when the air sharply changes its behaviour, for instance, passing from an open area into a tunnel, it will generate a significant variation

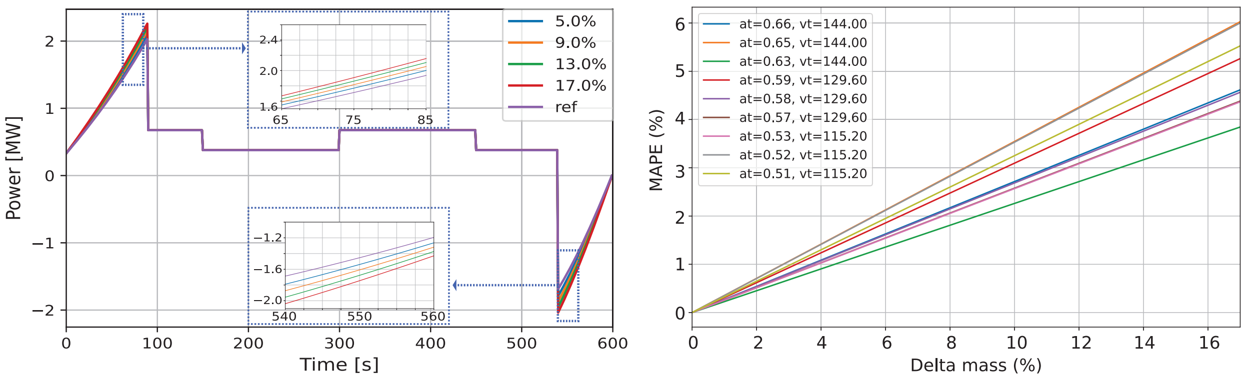


Fig. 5. Power estimation and MAPE for a single trip, considering $\Delta m = 5\%, 9\%, 13\%, 17\%$.

in the power demand. These effects become more noticeable when the vehicle is accelerating. The friction coefficient, on the other hand, is not related to neither the speed nor the acceleration, nevertheless, if the inclination is took into consideration, it can vary as well. Regarding the mass, despite it remains constant while the train is moving, it can be modified at each station. Assuming an average weight of 75 kg per person, and a total capacity of 250 passengers, the total mass of the system fluctuates between 5-17% with respect to the rated mass of the train, which is approximately 130 ton. For different scenarios, the model has a MAPE of about 2-3% and 1-2% at full and half capacity respectively. For the power demand profile, a simulation based on a specific section located between Wierden, Rijssen, Nijverdal and Almelo was done, considering Wierden as the principal node. In Fig. 6, a comparison between different assumptions for HVAC systems is presented, showing a variance up to 6% over the peak power values and about 5% over the average power consumption.

### B. Recoverable energy

Around $20-30\%$ of energy is potentially recoverable, nonetheless, for different scenarios regarding HVAC and over-voltage scheme at the catenary level also has an effect over

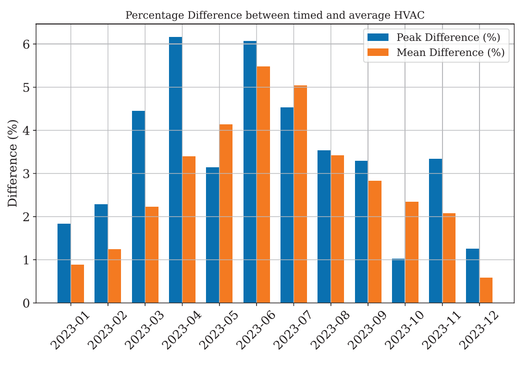


Fig. 6. Mean/Peak power comparison between different HVAC considerations.

power estimations, leading to different results. In this case, a chopper resistor is modeled for the over-voltage protection which is engaged when the voltage is over an specified threshold for each type of train. The recoverable energy can be obtained from the following power equivalence while the train is braking.

$$0 \leq P_{\text{REC}} = \begin{cases} (P_{\text{L}} - P_{\text{HVAC}}) & \text{if } V_L \leq V_{\text{THD}} \\ P_{\text{L}} - P_{\text{HVAC}} - P_{\text{BR}} & \text{otherwise} \end{cases}$$

Where $P_{\text{BR}}$ is the power through the chopper resistor. The results of the distribution of the recoverable energy for two different scenarios is presented in Fig. 7 with the outcome of the timed HVAC modeling on the left, and that of an average HVAC load profile assumption on the right. Recoverable energy varies about 1-2% when the utilization of the HVAC is more often, and up to 5.6% when the temperature increases, while the brake losses are kept as around the same percentage in both cases.

## IV. Conclusion

This paper addressed a sensitivity analysis for a DC traction power substation. The possible variations and assumptions in the traction parameters of the Davis equation has no significant effect over the power demand as the error in the energy modeling remains low (about 1-2% per trip). However, the effect of proper HVAC modeling over the energy demand has a notable impact. Two approaches for modeling HVAC system were presented, one with the actual on-max/off behavior of the system and the other with an average power profile. The results showed a difference in peak/average power consumption about 5% and between 2-6% in the recoverable energy calculations. These numbers could have a significant consequence on the design of the power converters and sizing of the distributed generation in the DC energy hub around a traction substation. Further works are encouraged on the topic of distributed generation modeling and the detailed modeling of the traction substation and its voltage and power profiles.

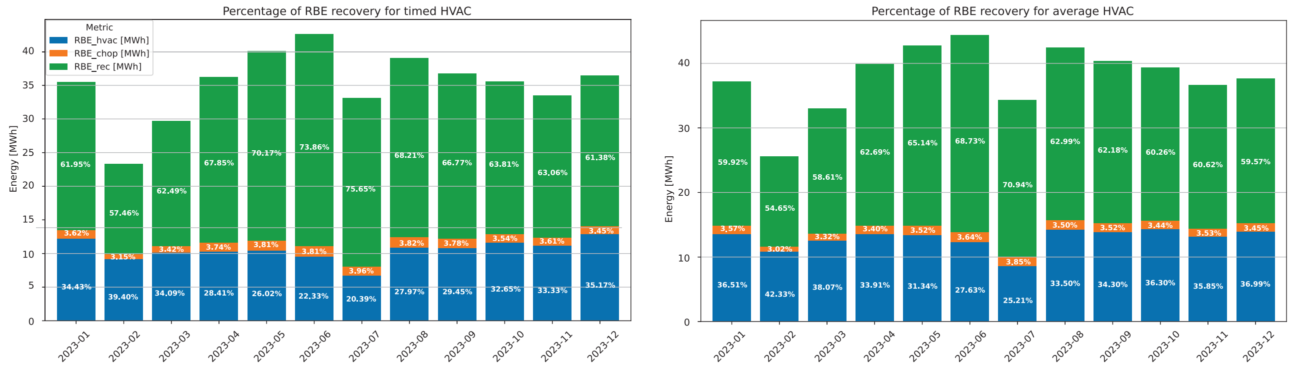


Fig. 7. Energy percentage usage from the total kinetic energy.

## Acknowledgment

The authors would like to thank the Europe's Rail program, Nederlandse Spoorwegen (NS) and ProRail working together to research feasible solutions for enhance the DC power system. This study is part of work package 11.1 of Rail4Earth, where similar pilots are build addressing different environments. The FP4 - Rail4EARTH project under Grant Agreement n°101101917 is supported by the Europe's Rail Joint Undertaking and its members.

## References

[1] A. Ipakchi and F. Albuyeh, "Grid of the future," *IEEE power and energy magazine*, vol. 7, no. 2, pp. 52–62, 2009.

[2] K. J. Dyke, N. Schofield, and M. Barnes, "The impact of transport electrification on electrical networks," *IEEE Transactions on Industrial Electronics*, vol. 57, no. 12, pp. 3917–3926, 2010.

[3] S. Rivera, S. M. Goetz, S. Kouro, P. W. Lehn, M. Pathmanathan, P. Bauer, and R. A. Mastromauro, "Charging infrastructure and grid integration for electromobility," *Proceedings of the IEEE*, 2022.

[4] S. Khayyam, F. Ponci, J. Goikoetxea, V. Recagno, V. Bagliano, and A. Monti, "Railway energy management system: Centralized–decentralized automation architecture," *IEEE Transactions on Smart Grid*, vol. 7, no. 2, pp. 1164–1175, 2015.

[5] M. Botte, L. D'Acierno, and M. Pagano, "Impact of railway energy efficiency on the primary distribution power grid," *IEEE Transactions on Vehicular Technology*, vol. 69, no. 12, pp. 14 131–14 140, 2020.

[6] I. Diab, G. R. C. Mouli, and P. Bauer, "A review of the key technical and non-technical challenges for sustainable transportation electrification: A case for urban catenary buses," in *2022 IEEE 20th International Power Electronics and Motion Control Conference (PEMC)*. IEEE, 2022, pp. 439–448.

[7] I. Diab, A. Saffirio, G. R. C. Mouli, A. S. Tomar, and P. Bauer, "A complete dc trolleybus grid model with bilateral connections, feeder cables, and bus auxiliaries," *IEEE Transactions on Intelligent Transportation Systems*, vol. 23, no. 10, pp. 19 030–19 041, 2022.

[8] J. A. Aguado, A. J. S. Racero, and S. de la Torre, "Optimal operation of electric railways with renewable energy and electric storage systems," *IEEE Transactions on Smart Grid*, vol. 9, no. 2, pp. 993–1001, 2016.

[9] J. Pouget, B. Guo, L. Bossoney, J. Coppex, D. Roggo, and C. Ellert, "Energetic simulation of dc railway micro-grid interconnecting with pv solar panels, ev charger infrastructures and electrical railway network," in *2020 IEEE Vehicle Power and Propulsion Conference (VPPC)*. IEEE, 2020, pp. 1–7.

[10] Y. Ge, H. Hu, J. Chen, K. Wang, and Z. He, "Combined active and reactive power flow control strategy for flexible railway traction substation integrated with ess and pv," *IEEE Transactions on Sustainable Energy*, vol. 13, no. 4, pp. 1969–1981, 2022.

[11] M. Brenna, F. Foiadelli, and H. J. Kaleybar, "The evolution of railway power supply systems toward smart microgrids: The concept of the energy hub and integration of distributed energy resources," *IEEE Electrification Magazine*, vol. 8, no. 1, pp. 12–23, 2020.

[12] E. P. de la Fuente, S. K. Mazumder, and I. G. Franco, "Railway electrical smart grids: An introduction to next-generation railway power systems and their operation." *IEEE Electrification Magazine*, vol. 2, no. 3, pp. 49–55, 2014.

[13] N. K. Panda, M. Poikilidis, and P. H. Nguyen, "Cost-effective upgrade of the dutch traction power network: Moving to bi-directional and controllable 3 kv dc substations for improved performance," *IET Electrical Systems in Transportation*, vol. 13, no. 2, p. e12084, 2023.

[14] D. Ronanki, S. A. Singh, and S. S. Williamson, "Comprehensive topological overview of rolling stock architectures and recent trends in electric railway traction systems," *IEEE Transactions on transportation Electrification*, vol. 3, no. 3, pp. 724–738, 2017.

[15] S. Su, Z. Tian, and R. M. Goverde, *Energy-Efficient Train Operation: A System Approach for Railway Networks*. Springer Nature, 2023.